



Numerical simulations of oscillations in solar corona excited by vortex shedding



Petr Jelínek¹, Sofya Belov¹, Marian Karlický², Maciej Zapiór²

¹University of South Bohemia, Faculty of Science, Department of Physics, Branišovská 1760, 370 05 České Budějovice, Czech Republic

²Academy of Sciences of the Czech Republic, v. v. i., Astronomical Institute, Fričova 258, 251 65 Ondřejov, Czech Republic

e-mail: pjelinek@prf.jcu.cz, belovs00@prf.jcu.cz, karlicky@asu.cas.cz, maciej.zapior@asu.cas.cz

Introduction

Wave and oscillatory phenomena are omnipresent throughout the whole solar atmosphere. They are the subject of theoretical and observational studies in association with the unsolved problem of heating of the solar corona and also the solar wind acceleration. The oscillations are interpreted in terms of magnetohydrodynamic (MHD) waves.

There exist many modes of oscillations, where transverse (kink) oscillations are one of the most studied wave phenomena in the solar atmosphere. They have been observed in coronal loops, solar prominences or flux ropes, which are often defined as clusters of magnetic field lines twisting around a common axis.

Nakariakov et al. (2009) present a model suggesting that a possible mechanism of the excitation of kink oscillations are coronal mass ejections (CME) causing the vortex shedding phenomenon. This phenomenon, which is well known and described in hydrodynamic conditions, consists in a periodic alternate formation of vortices from each of the two sides of a blunt flow obstacle, which can form a structured chain of vortices, called Kármán vortex street. The frequency of the process depends on the obstacle size and fluid velocity according to the Strouhal number. In the model mentioned above, the blunt obstacle is presented by the upper, horizontal section of a magnetic structure surrounded by vertical flow originating from a CME.

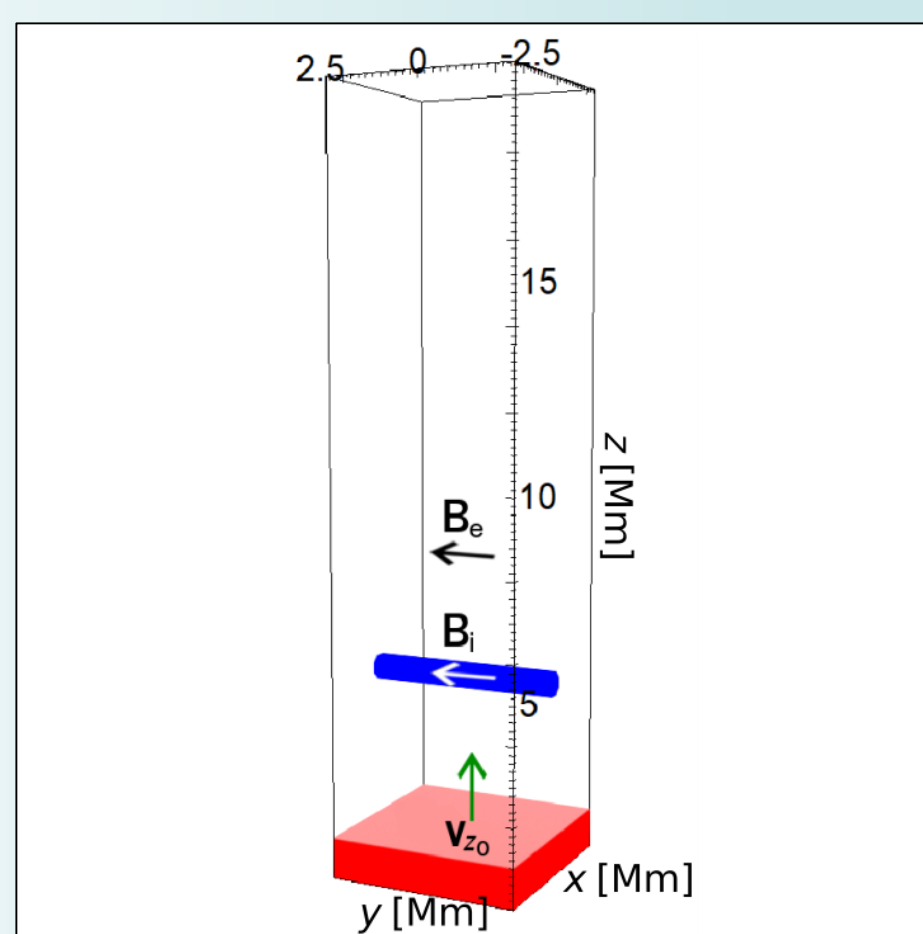


Figure 1: The sketch of the numerical box including its sizes. The blue cylinder represents the obstacle. The initial flow is denoted as v_{x0} .

Numerical model

The phenomenon of vortex shedding around a circular cylindrical obstacle was studied numerically by solving the MHD equations in three spatial dimensions using the Lare3d code. Our model mimics coronal mass ejection flowing around a dense and cold magnetic structure and leading to vortex shedding. Figure 1 illustrates the simulation box in the initial state and settings common to all performed simulations.

We consider two model cases: #1 – with a rigid and spatially fixed cylindrical obstacle, and #2 – with a flexible cylindrical obstacle fixed at boundaries, with only the y component of the magnetic field applied. In model case #1, the initial magnetic field is constant throughout the simulation box ($B_e = B_i = B$), but its value is different for each of the five simulations. All the initial parameters – see Tab. 1, are in conformity with the equilibrium condition.

Table 1: Physical parameters of the studied cases, where ρ_e and ρ_i are the initial external and cylinder mass densities, T_e and T_i are the initial external and cylinder temperatures, and B_e and B_i are the initial external and cylinder magnetic fields with only the y component.

	#1	#2
ρ_e	$10^{-12} \text{ kg} \cdot \text{m}^{-3}$	$10^{-12} \text{ kg} \cdot \text{m}^{-3}$
ρ_i	$10^{-11} \text{ kg} \cdot \text{m}^{-3}$	$10^{-11} \text{ kg} \cdot \text{m}^{-3}$
T_e	$2 \cdot 10^6 \text{ K}$	$2 \cdot 10^6 \text{ K}$
T_i	$2 \cdot 10^5 \text{ K}$	10^4 K
B_e	1 – 5 G	10 G
B_i	1 – 5 G	10.3 G

The gravitational field was not considered and the ideal MHD equations were used:

$$\frac{\partial \rho}{\partial t} + \nabla \cdot \rho \mathbf{v} = 0, \quad (1)$$

$$\rho \frac{\partial \mathbf{v}}{\partial t} + \rho(\mathbf{v} \cdot \nabla) \mathbf{v} + \nabla p - \frac{1}{\mu_0} (\nabla \times \mathbf{B}) \times \mathbf{B} = 0, \quad (2)$$

$$\frac{\partial p}{\partial t} + \mathbf{v} \cdot \nabla p + \gamma p \nabla \cdot \mathbf{v} = 0, \quad (3)$$

$$\frac{\partial \mathbf{B}}{\partial t} - \nabla \times (\mathbf{v} \times \mathbf{B}) = 0, \quad \nabla \cdot \mathbf{B} = 0, \quad (4)$$

where ρ is the mass density, \mathbf{v} is the flow rate, p is the gas pressure, \mathbf{B} is the magnetic field, μ_0 is the vacuum permeability and γ is the specific heat ratio.

Numerical results

Figure 2 shows the distribution of the y component of vorticity ω_y , which characterizes the vortex structure of the drag at each point of the continuum, given by the relation: $\omega = \nabla \times \mathbf{v}$, in the plane $y = 0$. The figures are shown for different magnetic fields from $B = 1 - 5$ G (left to the right) at time $t = 1120$ s. A structured chain of vortices, i.e. Kármán vortex street, can be seen in each panel. The panels in Fig. 3 show the dependence of the vortex shedding period and Strouhal number on the B value. In Fig. 4 we show the distribution of vorticity and gas pressure. We can clearly see the oscillations of the magnetic structure for different times of calculation. In Fig. 5 we estimated the period of these oscillations based on wavelet analysis of the wave signal.

Model case #1 – comparison of vorticity distribution

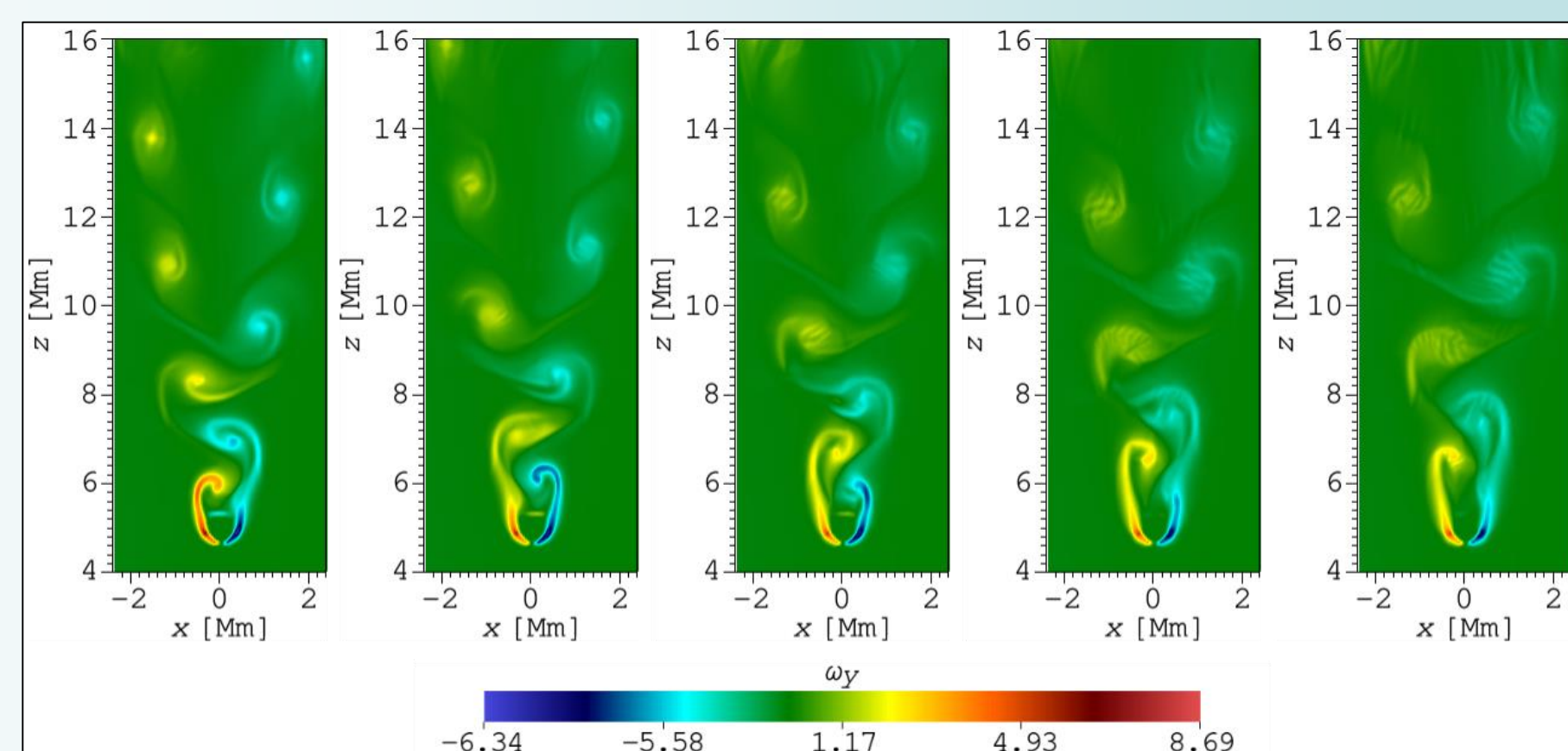


Figure 2: The set of figures showing the y component of vorticity ω_y , in arbitrary units, at time $t = 1120$ s for different values of the magnetic field. The strength of magnetic field is from 1 to 5 G (left to the right), respectively.

Model case #1 – comparison of the period and Strouhal number

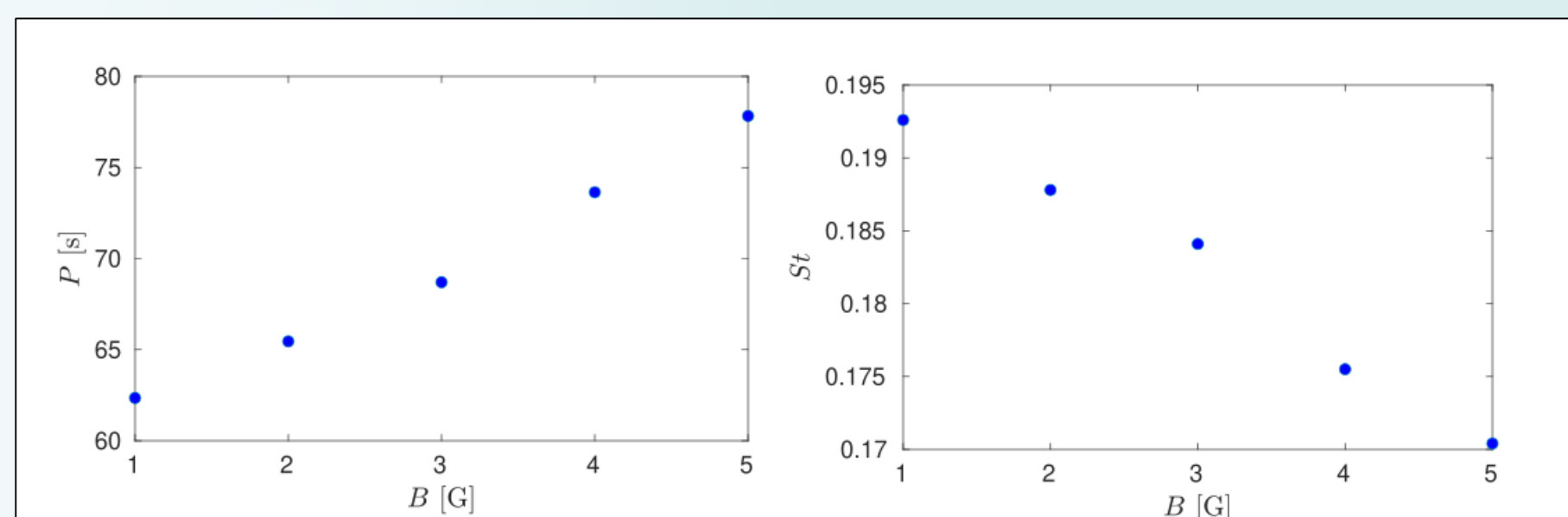


Figure 3: The dependence of vortex shedding period and Strouhal number on the value of the initial magnetic field.

Conclusions

We present the results from 3D MHD numerical simulations of transverse oscillations of a cylindrical structure performed using the code Lare3d. Two cases were numerically studied: #1 – flow around a "rigid" obstacle, which we studied parametrically to explore the creation of vortices for different magnetic field values and the dependence of Strouhal number on the magnetic field, and #2 – the vortex shedding phenomenon exciting transverse oscillations of a cylindrical structure that can freely move in all dimensions. The results obtained (oscillations with period approx. 20 – 80 s) can be interpreted as prominence/filament kink oscillations guided by a prominence fine structure as observed for example by Balthasar et al. (1993). They detected oscillations with a period of 30 s in spatially small areas of few arcsec in Doppler signal. Low period domain (below 5 minutes) of prominence oscillations is hard to explore because it requires high temporal cadence. Observations with high cadence are planned in the future using the HSA-2 instrument installed in Ondřejov Observatory. Numerical models, however, give us the possibility to study possible mechanisms of low-amplitude period oscillations.

Acknowledgement

The authors acknowledge support from the project 21-16508J of the Grant Agency of the Czech Republic.

Model case #2 – comparison of vorticity distribution and gas pressure distribution

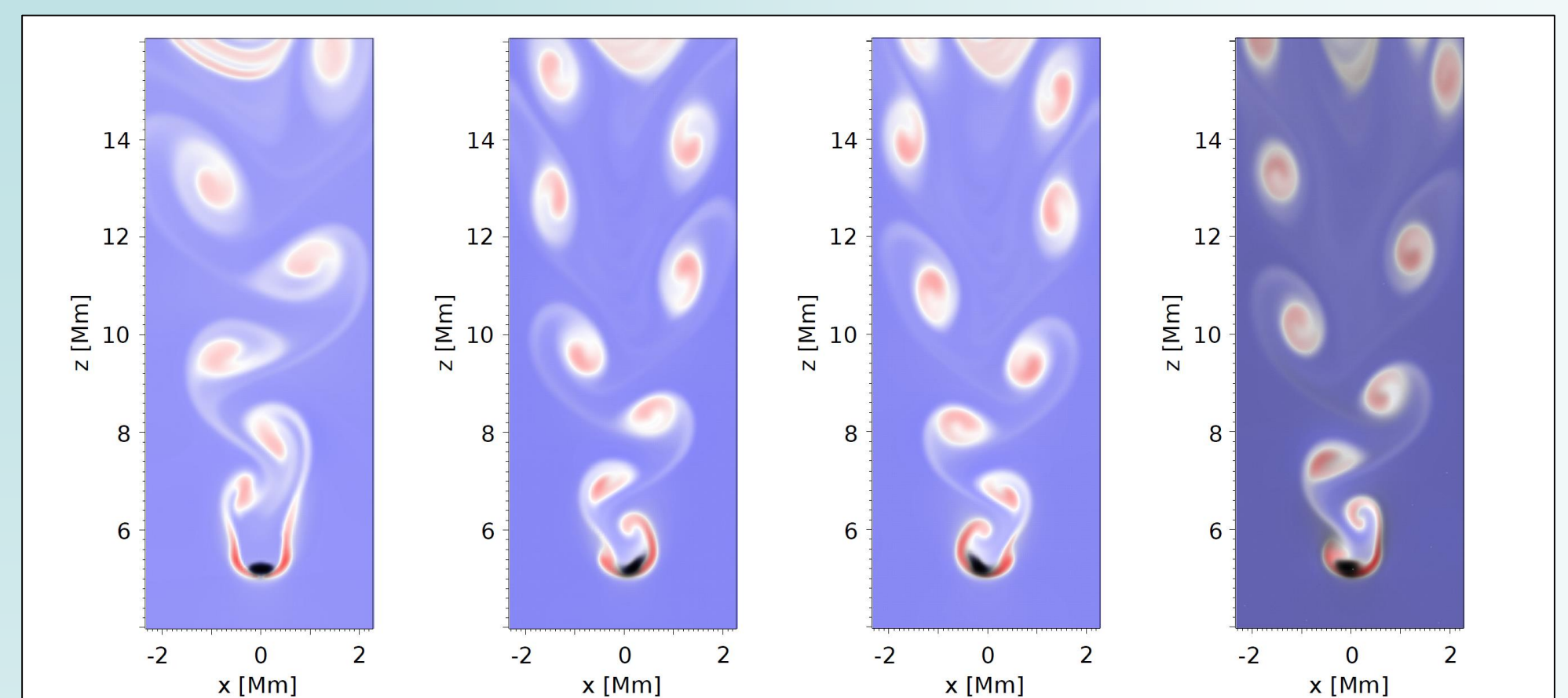


Figure 4: The time evolution of gas pressure (black area) and vorticity, showing the oscillations of the structure for times $t = 314; 388; 399$ and 526 s, respectively.

Model case #2 – wavelet analysis and period of oscillations

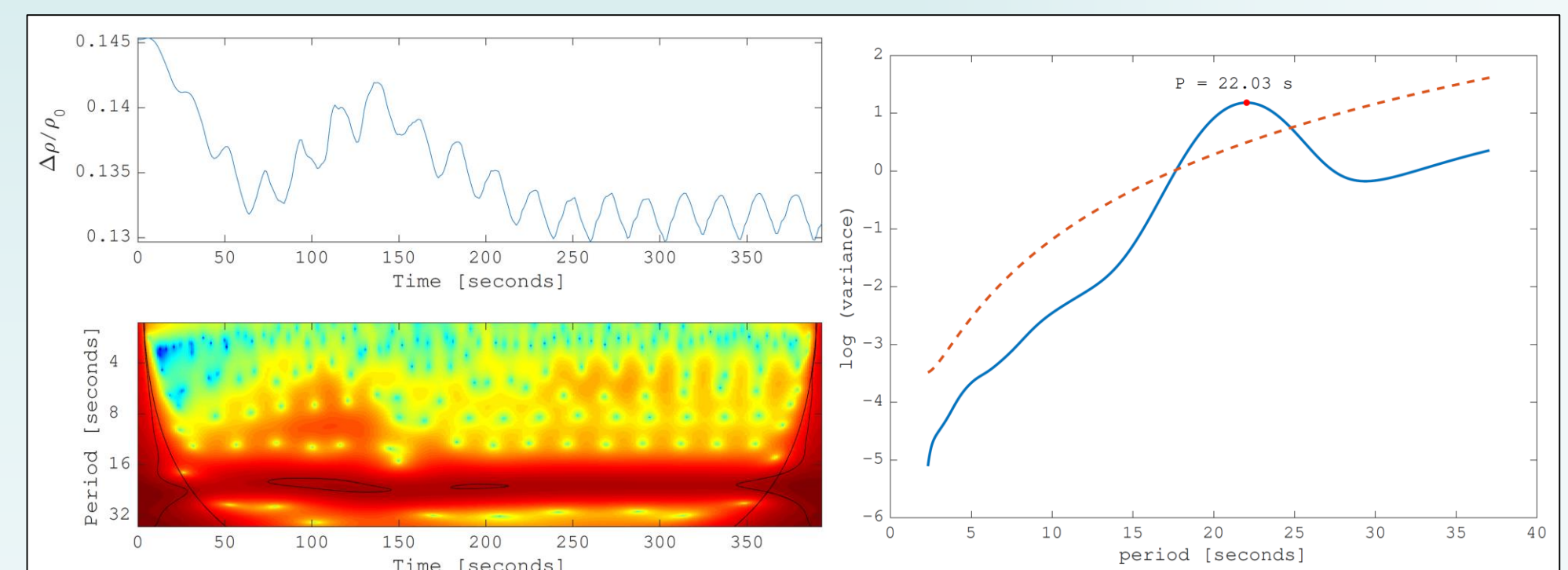


Figure 5: Wavelet analysis of the magnetic structure oscillations and estimated oscillation period.

References

Nakariakov, V., Aschwanden, M., Van Doorsselaere, T., A&A, **502**, 2, 661, 2009
Balthasar H. et al., A&A, **277**, 635, 1993